Access to Phosphorylation in Isocitrate Dehydrogenase May Occur by Domain Shifting[†,‡]

Janet Finer-Moore,[§,||] Susan E. Tsutakawa,[§,⊥] Diana B. Cherbavaz,[§,||] David C. LaPorte,[#] Daniel E. Koshland, Jr.,[⊥] and Robert M. Stroud*[,||]

Department of Biochemistry and Biophysics, University of California, San Francisco, California 94143-0448, Department of Biochemistry, University of California, Berkeley, California 94720, and Department of Biochemistry, University of Minnesota, Minneapolis, Minnesota 55455

Received May 19, 1997; Revised Manuscript Received July 24, 1997[⊗]

ABSTRACT: To clarify further the mechanism of regulation by phosphorylation of isocitrate dehydrogenase, cocrystallization of isocitrate dehydrogenase and isocitrate dehydrogenase kinase/phosphatase in the presence of an ATP analog was attempted. Although cocrystallization was unsuccessful, a new crystal form of isocitrate dehydrogenase was obtained which provides insight into the phosphorylation mechanism. The new, orthorhombic crystal form of isocitrate dehydrogenase is related to the previously reported tetragonal form largely by an ∼16° shift of a large domain relative to the small domain and clasp region within each subunit of the dimeric enzyme. The $NADP^+$ cofactor binding surface is significantly disrupted by the shift to the open conformation. The solvent-accessible surface area and surface-enclosed volume increase by 2% relative to the dimeric tetragonal form. Most of the increase results from expansion of the active site cleft such that the distance across its opening increases from approximately 5 to 13 Å, significantly increasing accessibility to Ser-113. The conformation of isocitrate dehydrogenase in the orthorhombic crystal form more closely resembles that of the crystal structure of the homologous enzyme 3-isopropylmalate dehydrogenase than does the tetragonal isocitrate dehydrogenase conformation. Since the crystal lattice forces are fairly weak, it appears that isocitrate dehydrogenase is a flexible molecule that can easily undergo domain shifts and possibly other induced fit conformational changes, to accommodate binding to isocitrate dehydrogenase kinase/phosphatase.

$NADP^+$-dependent isocitrate dehydrogenase (IDH, EC 1.1.1.42) catalyzes the oxidative decarboxylation of isocitrate to produce α-ketoglutarate in the Krebs cycle (Stryer, 1988). In plants and bacteria, enzymes of an alternate metabolic pathway, the glyoxalate shuttle, are induced when the nutrient conditions are deficient and acetate is the sole carbon source (LaPorte et al., 1985). When the glyoxylate shuttle is utilized, IDH is found to be phosphorylated (Garnak & Reeves, 1979) and completely inactivated by the phosphorylation (LaPorte & Koshland, 1982). This phosphorylation occurs at a serine residue (Nimmo & Nimmo, 1984) at the active site (Hurley et al., 1990a) unlike most other regulatory phosphorylations that occur at allosteric sites (Hurley et al., 1990a; Stroud, 1991).

The crystal structure of dephosphorylated isocitrate dehydrogenase at 2.5 Å resolution (Hurley et al., 1989) was initially determined from a tetragonal crystal form. The phosphorylated form is isomorphous with active enzyme and shows that phosphorylation does not induce any significant or long-range positional changes in the IDH structure (Hurley et al., 1990b). Phosphoserine at position 113 blocks isocitrate binding primarily by electrostatic repulsion and secondarily by steric effects (Hurley et al., 1990a) (Dean & Koshland, 1990). However, the X-ray structures indicate that the site of phosphorylation (Ser-113) at the active site is relatively sequestered and inaccessible, leaving the question of how the IDH kinase/phosphatase (IDH K/P) (LaPorte & Koshland, 1982) could reach this site and catalyze the transfer of phosphate from ATP to serine 113 or remove phosphate from phosphoserine 113 since there is not enough room for insertion of a protein (Hurley et al., 1990a). Two models for how this might occur seem apparent. IDH K/P could induce a conformational change around residue 113 in order to bind to and transfer a phosphate to that residue in a different conformation. Alternatively, a spontaneous conformational change could occur to a form of IDH that would render Ser-113 accessible.

In order to resolve how the mechanisms of phosphorylation and dephosphorylation occur, we crystallized another crystal form of IDH that has turned out to throw light on the question of the accessibility of the serine to phosphorylation.

EXPERIMENTAL PROCEDURES

A previously unobserved crystal form of IDH was obtained during trials aimed at crystallizing a complex of IDH with

[†] This work was supported by National Institutes of Health Grant GM24485 (to R.M.S.), National Institutes of Health Grant DK40486 (to D.C.L.), the W. M. Keck Foundation and National Institutes of Health Grant DK09765 (to D.E.K.), and American Cancer Society Fellowship PF-3657 (to D.B.C.).

[‡] Atomic coordinates have been deposited in the Brookhaven Protein Data Bank. The access code is 1SJS.

[§] The first three authors contributed to the work as follows: S.E.T. prepared the isocitrate dehydrogenase used in the crystallization trials, D.B.C. grew the crystals, collected and processed the X-ray data, and contributed Figure 4 and the associated discussion, and J.F.-M. solved and refined the crystal structure.

[||] University of California, San Francisco.

[⊥] University of California, Berkeley.

[#] University of Minnesota.

[⊗] Abstract published in *Advance ACS Abstracts,* October 1, 1997.

[1] Abbreviations: IDH, isocitrate dehydrogenase; IMDH, 3-isopropylmalate dehydrogenase; IPM, 3-isopropylmalate; IDH K/P, isocitrate dehydrogenase kinase/phosphatase; rms, root mean square.

S0006-2960(97)01169-0 CCC: $14.00

the IDH K/P. Dimeric IDH (43 kDa/subunit) and dimeric IDH K/P (68 kDa/subunit) were combined in a 2:1 molar ratio and concentrated to 5−8 mg/mL in an exchange buffer consisting of 100 mM NaCl, 100 mM Hepes, 50 μM ATPγS, 50 μM $MgCl_2$, 2 mM DTT, and 0.01% NaN_3, at pH 7.4. Crystals were grown by vapor diffusion against a solution of 29−32% PEG 4K, 10−90 mM ammonium acetate, 2 mM DTT, and 50 mM Tris-HCl, at pH 8.5, from drops containing 50% by volume of the protein solution and 50% of the precipitant solution. This method produced crystals that were approximately 0.08 mm in the longest dimension. Macroseeding of crushed crystals further increased crystal dimensions to a maximum of 0.15−0.2 mm in the longest dimension. IDH did not crystallize under the same crystallization conditions in the absence of IDH K/P. It is not clear whether the presence of IDH K/P itself or of some unknown contaminant, such as a trace amount of a metal ion, promoted the new crystal form.

The crystals were orthorhombic, space group $C222_1$, with cell constants $a = 124.5$ Å, $b = 77.5$Å, and $c = 92.1$Å, too small to accommodate a complex of IDH with IDH K/P in the asymmetric unit. The previously determined tetragonal crystal form has cell dimensions $a = b = 105.1$ Å, and $c = 150.3$ Å. The orthorhombic crystals contain one protomer of dimeric IDH per asymmetric unit, with the molecular 2-fold axis coincident with a crystallographic 2-fold. The solvent content is 50%.

X-ray intensities were measured at room temperature for three crystals at the Stanford Synchrotron Radiation Laboratory on beamline 7-1, using a MAR image plate, 1.08 Å radiation, and 2° or 3° frames. Intensities were integrated using the program DENZO and scaled using Scalepack (Otwinowski, 1993). Frames which had R_{sym}'s of greater than 10%, or otherwise showed evidence of crystal decay, were not included in the merged data set. A total of 37 773 observations of 13 757 reflections between 50 and 2.42 Å resolution were processed. The overall $R_{sym} = \Sigma|I - \langle I\rangle|/\Sigma I$ for the data was 7.5%.

A molecular replacement solution was obtained by application of the Crowther rotation function (Crowther, 1972) and an *R*-factor translation search, using a dimer of IDH [previously solved in a tetragonal unit cell (Hurley et al., 1989)] for the search model, and data between 10 and 4.5 Å resolution. In the best scoring molecular replacement solution, the dimer 2-fold axis of IDH was aligned along a crystallographic 2-fold [(0, *Y*, $^1/_4$)], as required by the unit cell volume. Interpenetration of symmetry-related molecules at one crystal contact required manual rebuilding of a segment of the protein using CHAIN (Sack, 1988). The manually adjusted structure was refined by simulated annealing as implemented in X-PLOR (Brunger et al., 1987), which decreased the *R*-factor to 33% but did not decrease R_{free} (Brunger, 1992) from its initial value of 48%, suggesting that a conformation of the structure differed from that of the search molecule. $(2F_o - F_c)\alpha_{calc}$ density was uniformly good for residues 126−317, the small and the clasp domains of IDH (Hurley et al., 1989), but the remaining residues that constitute the large domain of IDH were in broken density. We therefore suspected a domain shift in the orthorhombic crystal form of IDH compared to the search model. Rotation solutions were separately determined for the large domains of the IDH dimer and for the small/clasp domains by molecular replacement using AMORE (Navaza, 1994). In each case, the peak height of the rotation function at the optimum solution was twice the value at the second highest peak. A translation solution for the large domain was determined, and a fixed contribution to F_c's from the properly positioned large domain was included in the translation search for the small/clasp domains.

Table 1: Crystallographic Data for IDH

unit cell lengths (Å)	124.5, 77.5, 92.1
space group	$C222_1$
maximum resolution (Å)	2.42
no. of observations	37773
no. of reflections	13753
$R_{merge\ (\%)}$	7.5
no. of atoms per asymmetric unit	3268
no. of waters	90
resolution for refinement (Å)	7.0−2.42
data cutoff (σ)	0
data completeness (%)	69
$R_{crys\ (\%)}$	18.1
$R_{free\ (\%)}$	24.8
rms deviation, bonds (Å)	0.005
rms deviation, angles (deg)	1.25
rms deviation, torsions (deg)	23.2
average atomic *B*-factor (Å^2)	24

The molecular replacement solutions for both fragments were consistent with each other and could be rejoined manually by adjusting just two or three residues. The crystallographic *R*-factor for data from 10 to 3 Å resolution for the joined fragments was 32%. Manual rebuilding of a region of the protein at a crystal contact, followed by rigid-body, positional, and restrained individual *B*-factor refinements (Brunger et al., 1987), gave an *R*-factor = 20.4% and $R_{free} = 26.9\%$ for data between 7 and 2.4 Å. R_{free} decreased with each step of refinement. Manual adjustment of side chains and addition of ordered water to the structure decreased the *R*-factor to 18.1% and R_{free} to 24.8%. As in the tetragonal crystal structure, the N-terminus is disordered and residue Met-1 was not located. Residue Glu-2 was refined as alanine. At the current state of refinement 96% of the side chains adopt one of their commonly observed conformations (Ponder & Richards, 1987). Most residues are in allowed regions of the Ramachandran diagram, although there is one outlier, Arg-96 ($\phi = 65°$, $\psi = -45°$), that is nevertheless in excellent density in $(2F_o - F_c)\alpha_{calc}$ maps. Crystallographic data are listed in Table 1.

The shift in orientation of the large domain of IDH with respect to the small/clasp domains, seen between the earlier tetragonal and the present orthorhombic crystal structures, was assessed by first overlapping the small and clasp domains of the two structures using a least-squares procedure. After the small domains had been overlapped, the relative orientations of the large domains were quantitatively compared by calculating the angles between their respective principal axes, as described in Browner et al. (1992) using the program GEM (Fauman et al., 1994) . Similarly, the small domain of the homologous enzyme 3-isopropylmalate dehydrogenase (IMDH) was overlapped with each crystal form of IDH, and the relative orientations of conserved regions of the large domain in IMDH and the large domains in both crystal forms of IDH were quantitatively compared. The accessibility of Ser-113 to probe spheres of varying radii was measured using the program SURFACE, written by Mark Handschumacher and F. M. Richards.

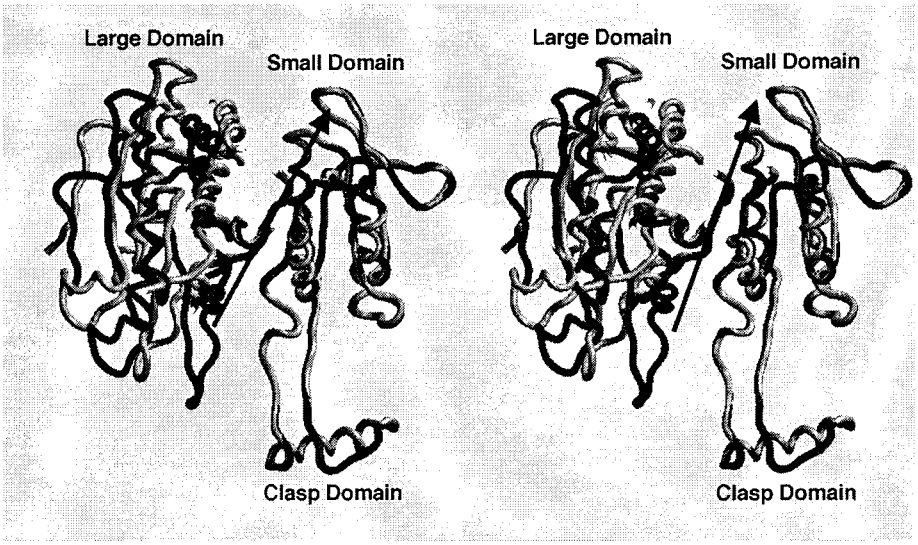

FIGURE 1: Divergent stereoview of a section through the α-carbon tracing (in gray) of a protomer of IDH as it appears in the orthorhombic crystal structure, superimposed on the α-carbon tracing (in black) of a protomer of IDH as seen in the tetragonal crystal structure (Hurley et al., 1989). The two structures were superimposed by overlap of their small domains. The axis of rotation that relates the orientations of the large domains coincides approximately with β-strand F and is indicated by the arrow. The figure was made using SETOR (Evans, 1993).

RESULTS

Rigid Body Rotation of the Large Domain Makes the Phosphorylation Site More Accessible. The conformation of IDH in the orthorhombic crystal structure differs from its conformation in the previously determined tetragonal crystal structure primarily by an ~16° rotation of the large domain with respect to the small and clasp domains of a subunit (Figure 1). The domain rotation opens up the active site cleft, exposing Ser-113. Ser-113 is accessible to a probe sphere of up to 5 Å in radius in the orthorhombic form, while in the tetragonal form it is only accessible to a probe sphere of up to 2.5 Å radius.

The rms deviations between the main chain coordinates of the large domains, and the small domains/clasp regions of the two crystal structures, when aligned separately, are 0.61 and 0.37 Å, respectively. The axis of rotation for the rigid-body shift approximately coincides with β-strand F at the interface between the large and small domains of the protein. β-Strand F lies at the center of the 12-stranded core β-sheet that spans the two domains. The domain rotation is typical of hinge motions used by other proteins to open and close their active sites (Gerstein et al., 1994) and does not involve rearrangement of hydrogen bonds within the β-sheet. It is accompanied by ~25° rotations in the (ϕ,ψ) angles for residues Cys-127 and Leu-128 in the center of β-strand F, as well as (ϕ,ψ) changes of 25° or more in 15 other residues, most of which lie in loops at the edges of the large domain side of the β-sheet (Table 2).

The orthorhombic crystal form of IDH was obtained in the absence of ligands. There is no extra density in the active site to suggest that the phosphorylation site has been modified or that anything other than ordered water molecules are bound. Therefore, we conclude that the new conformation of IDH is an easily accessible, low-energy conformation, stabilized by crystal contacts in the orthorhombic cell. Thus the alternate conformations of IDH appear to be energetically similar, suggesting that IDH can easily undergo an induced fit conformational change on binding of the kinase/phosphatase.

Table 2: Listing of (ϕ,ψ) Angles for Residues with (ϕ,ψ) Angles That Change by at Least 25° during the IDH Domain Shift[a]

residue	(ϕ,ψ), closed IDH	(ϕ,ψ), open IDH	(ϕ,ψ), IMDH
20	−122, 131	−104, 159	
33	−53, −45	−79, −38	
60	−73, −38	−74, 11	
63	−78, 135	−105, 141	
79	119, 166	177, −103	
80	−24, −67	−157, −60	
96	60, −13	65, −45	
97	−160, 129	−121, 145	
103	−133, 130	−115, 158	
127 (102)	**−107, 106**	**−99, 132**	**−102, 132**
128 (103)	**−97, 117**	**−124, 123**	**−119, 124**
321	−101, 0	−68, −12	
350	−126, −20	−100, −50	
397	−130, 163	−126, 126	
398	−115, 137	−82, 129	
399	70, 42	96, 9	
400	−118, 152	−80, 146	

[a]Residues 127 and 128 and the corresponding residues in IMDH are listed in bold type. IMDH residue numbers are given in parentheses after the IDH numbers. IDH residues 127 and 128 (and residues 102 and 103 in IMDH) probably transmit domain movement.

Aside from isolated residues (Table 2) that exhibit large changes in their (ϕ,ψ) angles due to domain shift, there are two regions of the orthorhombic IDH form whose conformation is influenced by crystal packing. These include residues 182−187 in the clasp domain and residues 106−112, the loop immediately preceding the IDH phosphorylation site. Residues 106−112 were rebuilt into density to avoid unreasonably close contacts between symmetry-related molecules and were the only residues whose backbone had to be manually rebuilt during refinement. They remain highly disordered and reside in broken density. Neither simulated annealing refinement nor calculation of omit maps helped to better define this part of the structure. The change in structure and increase in mobility of this loop may serve to stabilize the open conformation of the protein present in the orthorhombic crystals.

Substrate Binding May Induce Further Conformational Changes. In the tetragonal form, hydrogen bonding via

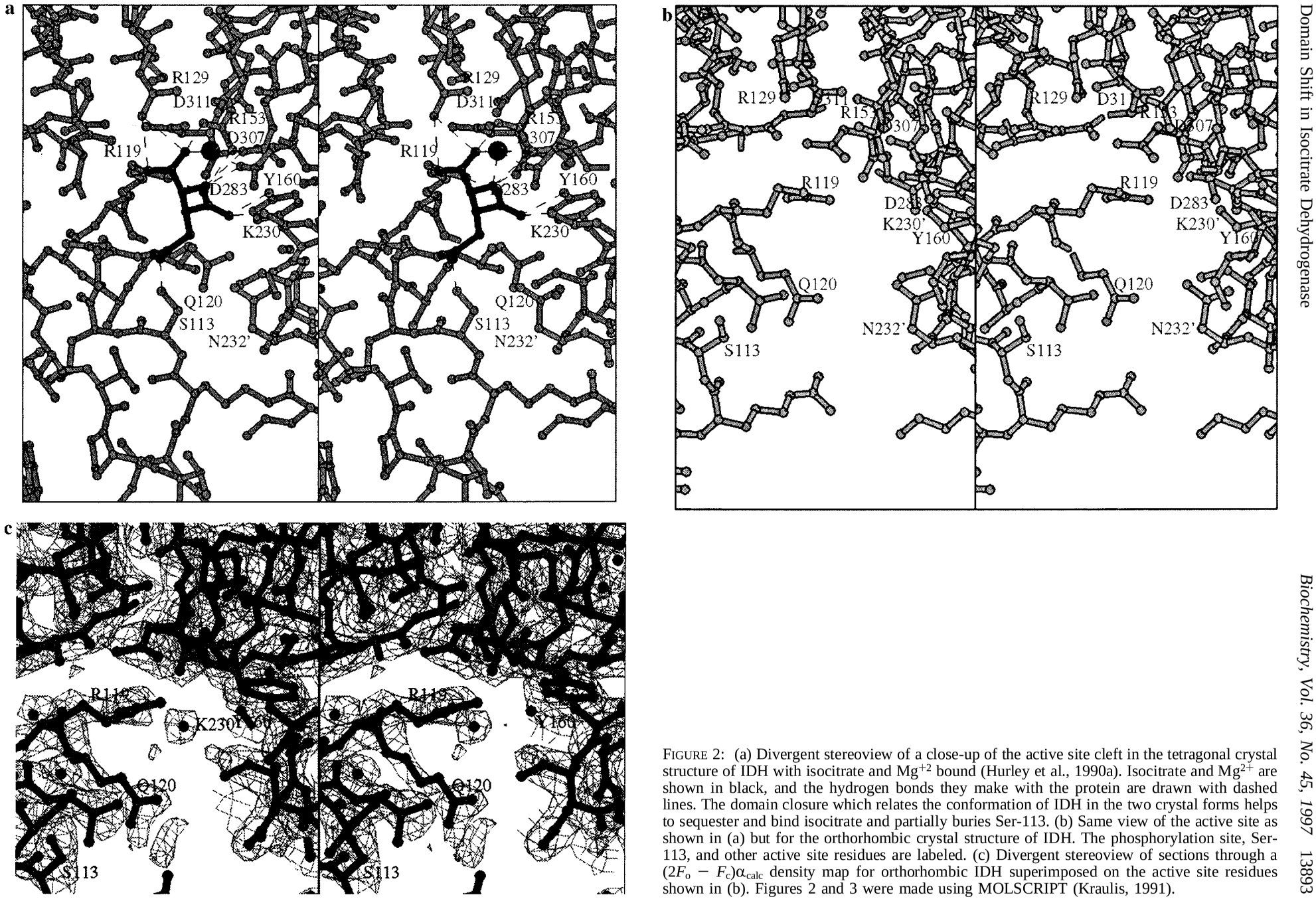

FIGURE 2: (a) Divergent stereoview of a close-up of the active site cleft in the tetragonal crystal structure of IDH with isocitrate and Mg^{+2} bound (Hurley et al., 1990a). Isocitrate and Mg^{2+} are shown in black, and the hydrogen bonds they make with the protein are drawn with dashed lines. The domain closure which relates the conformation of IDH in the two crystal forms helps to sequester and bind isocitrate and partially buries Ser-113. (b) Same view of the active site as shown in (a) but for the orthorhombic crystal structure of IDH. The phosphorylation site, Ser-113, and other active site residues are labeled. (c) Divergent stereoview of sections through a $(2F_o - F_c)\alpha_{calc}$ density map for orthorhombic IDH superimposed on the active site residues shown in (b). Figures 2 and 3 were made using MOLSCRIPT (Kraulis, 1991).

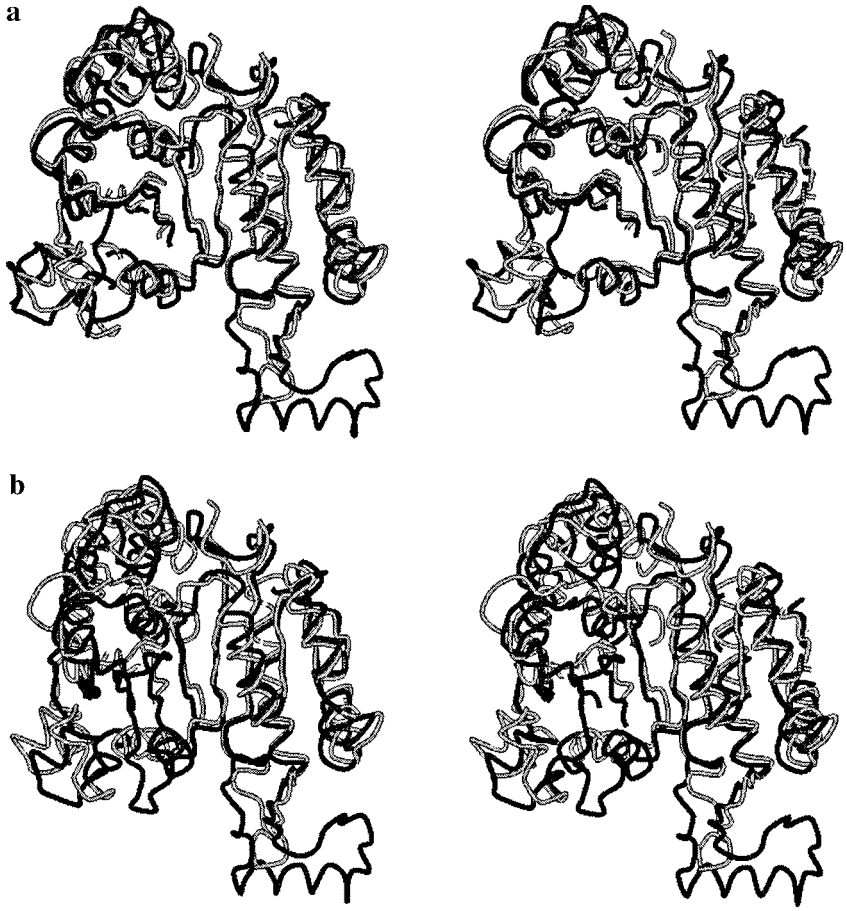

FIGURE 3: (a) Divergent stereoview of a section through the α-carbon tracing of the orthorhombic IDH protomer (in black) superimposed with the α-carbon tracing of the crystal structure of the IMDH protomer (Imada et al., 1991) (in gray). (b) Same section as in (a) through the α-carbon tracing of tetragonal IDH (in black) superimposed with the α-carbon tracing of the crystal structure of IMDH (in gray). IMDH was overlapped with each IDH by least-squares fit of the main chain atoms of their small domains. The active site of IMDH is in an "open" conformation more similar to that seen in orthorhombic IDH than in tetragonal IDH.

ligand, isocitrate, bridges the large and small domains (Figure 2a), presumably shifting the equilibrium toward the closed conformation. This ligand-mediated hydrogen-bonding network cannot occur in the orthorhombic form as the same protein residues are too far apart (Figure 2b). The $NADP^+$ cofactor binding surface (Hurley et al., 1991; Stoddard et al., 1993) is also disrupted in the orthorhombic form. The tight turn formed by residues 320−323 is the transition region between the large and small domains and flanks the adenine binding pocket. This turn moves away from the nucleotide binding site to accommodate domain shift in orthorhombic IDH. Thus, $NADP^+$ association favors the closed form of IDH. The binding surface for the proton recipient end of the cofactor, the nicotinamide moiety, is intact, but the majority of nicotinamide−active site interactions are mediated through isocitrate. Since isocitrate binding is disrupted and the ligand is unable to bind the open form, the nicotinamide interactions are disturbed in the active site as well.

The homologous enzyme, 3-isopropylmalate dehydrogenase (IMDH), crystallizes in an open conformation similar to that seen in the orthorhombic IDH crystal structure (Imada et al., 1991) (Figure 3). IMDH binds a similar substrate, isopropyl malate (IPM), and, like IDH, requires a pyridine nucleotide, NAD^+ in this case, and either Mg^{+2} or Mn^{+2} for the dehydrogenation and decarboxylation reactions. Small-angle X-ray scattering from solutions of IMDH in the presence of ligands shows that on complex formation IMDH becomes much more compact (Kadono et al., 1995). The radius of gyration and intraparticle distance distribution for the ternary complex of IMDH, NADH, and IPM are consistent with a closed conformation resembling that of IDH in tetragonal crystal structures. Binary complexes with either IPM or NADH adopt conformations intermediate between open and closed. Yet, in spite of large conformational changes seen in solution structures of IMDH complexes, all crystal structures of IMDH, liganded or unliganded, occur in the same open conformation. In contrast, IDH typically crystallizes in a fully closed conformation, even in the absence of ligands.

After alignment, the rms deviation between the main chain coordinates of the large domains of tetragonal IDH and IMDH (excluding inserts) is 2.3 Å, and the rms deviation between main chain coordinates of the small domains after alignment is 1.5 Å. Thus the two enzymes have similar crystal structures whose domains are related by domain rotations. The conformational differences between IMDH and tetragonal IDH can be described by a 22° rotation about an axis coincident with β-strand F followed by an ∼20° rotation of the large domain about an axis in the plane of the β-sheet, perpendicular to β-strand F (Figure 3b). The rotation about the axis coincident with β-strand F is equivalent to the rotation describing the domain shift between open and closed forms of IDH and correlates with large (ϕ,ψ) angle differences between residues C127, L128 in IDH and the equivalent residues N102, L103 in IMDH (Table 2).

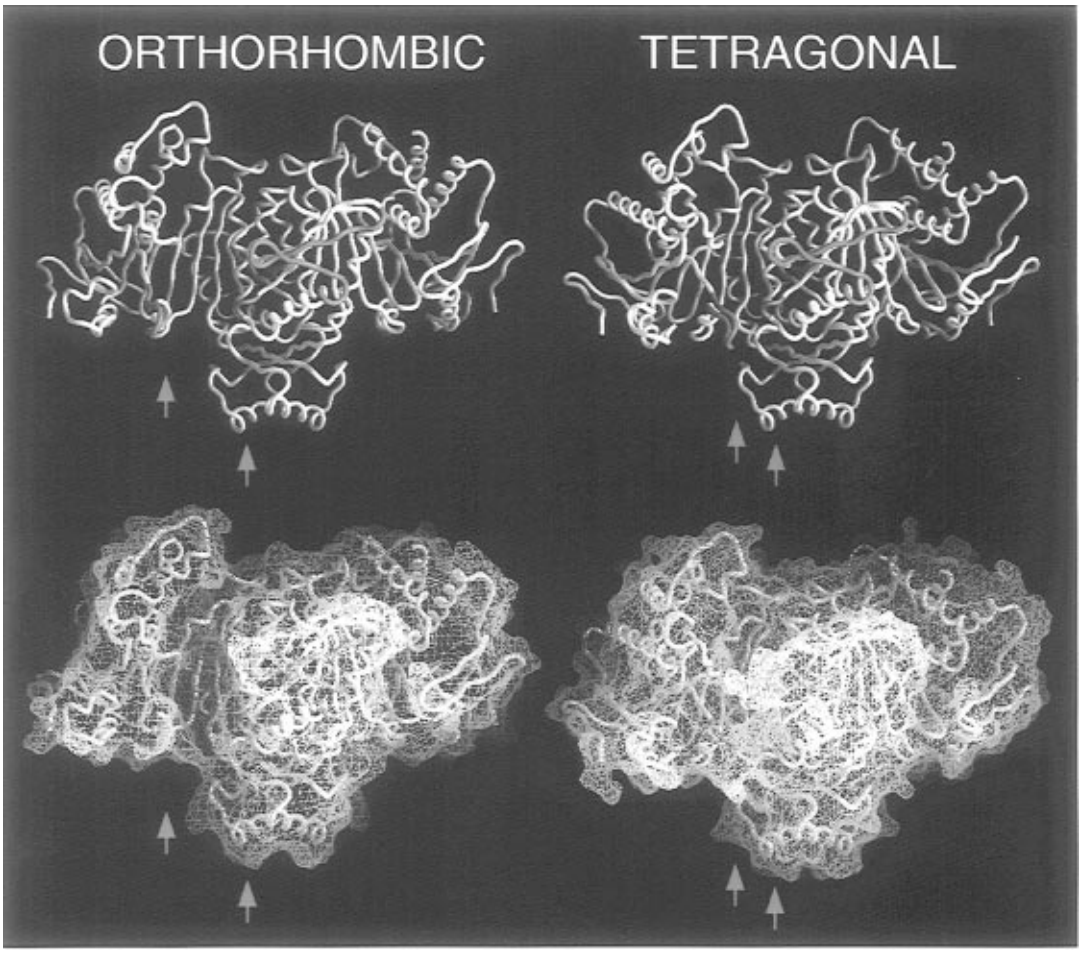

FIGURE 4: Views of the active site clefts and the solvent-accessible surfaces of the open (orthorhombic) and closed (tetragonal) form of dimeric IDH. The residue backbones of the phosphorylation loop (residues 105−114), residues 231−233 (across the active site cleft from Ser-113), and the coil between β-strands K and L are highlighted in orange. The distance across the active site cleft between residues Ser-113 and Asn-232 decreases from 13 to 5 Å in the transition between open and closed forms. Ser-113 (left arrow) is more exposed in the open form than in the closed form. The solvent-accessible surface representations (structures in lower panels) illustrate the constriction of the active site cleft by a segment of the small domain of the tetragonal form relative to the orthorhombic form. IDH is shown as the dimer, which is the catalytically active form. The top and bottom pairs are of identical views. This figure was prepared with GRASP (Sridharan et al., 1995) molecular modeling software.

The IDH active site in the orthorhombic crystal structure is almost as open as that of IMDH (Figure 3a). The conformation of IMDH is related to the open conformation of IDH by a rotation of just 6° about the axis coincident with β-strand F and a 20° rotation about an axis perpendicular to strand F. The (ϕ,ψ) angles for N102 and L103 are (−102, 132) and (−119, 124), respectively, very similar to the (ϕ,ψ) angles of the analogous residues C127 and L128 in IDH (Table 2). Thus we postulate that a conserved domain rotation occurs in IMDH and IDH, illustrated by the two crystal forms of IDH, and that the rotation may be transmitted by local conformational changes at C128, L128 (N102, L103 in IMDH). The conserved domain shift provides a mechanism for sequestering ligands in the active site of IDH or IMDH (Figure 2). These results suggest that both open and closed conformations are possible for IMDH and IDH, and the energy difference between these conformations is small. Apparently, the equilibrium between open and closed states can be influenced by crystal packing and by ligand binding.

DISCUSSION

In IDH, domain shift allows IDH K/P a mechanism for opening the active site cleft, making easier the regulation by phosphorylation at Ser-113. In the orthorhombic crystal form, Ser-113 is 13 Å across the active site to its nearest neighbors, Asn-232 or Ile-233, and is accessible to a probe sphere of radius 5 Å; in the tetragonal form, Ser-113 and Asn-232 or Ile-233 are 4−5 Å apart, and Ser-113 is only accessible to probes of up to 2.5 Å radius (Figure 4, top). Calculations of the surface area and volume of the two different dimeric forms reveal that both parameters, area and volume, of the orthorhombic form increase by 2% relative to the tetragonal form. Much of that increase resides in the expansion of the active site cleft, and qualitative comparison of both dimeric forms verifies the increase (Figure 4, bottom). A notable change in the dimeric forms of IDH is that the coil between β-strands K and L (Figure 4) appears to shield the active site and nearly covers the phosphorylation site when the large domain is in the closed conformation. Expansion of the active site cleft in the open form can therefore allow dimeric 136 kDa IDH K/P access to sequestered Ser-113.

The existence of two forms of IDH indicates the flexibility of the protein. Binding of IDH K/P probably induces conformational changes, and these further conformational changes make access to Ser-113 possible. These changes

could include, for example, a larger domain shift or local conformational changes in the loop containing residues Pro-106−Ser-113. Residues 106−112 are disordered in the orthorhombic ("open") crystal structure, indicating that the loop containing Ser-113 is mobile when IDH is in the newly obtained open conformation reported here.

The substrates of IDH (e.g., isocitrate, $NADP^+$) may control the phosphorylation cycle by stabilizing closed conformations of IDH. If so, NADP(H) should inhibit both IDH kinase and IDH phosphatase because this ligand binds to both phospho- and dephospho-IDH. In contrast, isocitrate should only inhibit IDH kinase because it does not bind to phospho-IDH. Consistent with this model, NADP(H) and isocitrate inhibit IDH kinase. Furthermore, NADP(H) inhibits IDH phosphatase but isocitrate does not (LaPorte, 1993; LaPorte & Koshland, 1983; Miller et al., 1996). Recent studies on the regulation of IDH K/P are also consistent with our model (unpublished results). For IDH kinase, isocitrate and NADP(H) appeared to be competitive with dephospho-IDH, suggesting that these ligands blocked IDH binding. Similar results were obtained for NADP(H) inhibition of IDH phosphatase. These effects appear to result from binding of these ligands to the active site of IDH. Amino acid substitutions which reduce the affinity of this site for isocitrate had parallel effects on the ability of isocitrate to inhibit IDH kinase. Similarly, mutations which changed the specificity of IDH from NADP(H) to NAD(H) had the same effect on the regulation of IDH kinase and IDH phosphatase by these dinucleotides (Chen et al., 1995; unpublished results).

The new orthorhombic crystal form of IDH therefore uncovers a key conformational transition. Ironically, a failed attempt to cocrystallize IDH with IDH K/P resolved the previous dilemma of how IDH is phosphorylated. In this model, phosphorylation can occur only after a conformational change in IDH to a more open conformation. Our results suggest that IDH may exist as an equilibrium between energetically similar open and closed forms. We propose that IDH K/P selectively binds to open conformations of IDH, perhaps inducing even further conformational changes to position Ser-113 in its active site.

REFERENCES

Browner, M. F., Fauman, E. B., & Fletterick, R. J. (1992) *Biochemistry 31*, 11297−11304.
Brunger, A. T. (1992) *Acta Crystallogr., Sect. D D49*, 24−36.
Brunger, A. T., Kuriyan, J., & Karplus, M. (1987) *Science 235*, 458−460.
Chen, R., Greer, A., & Dean, A. M. (1995) *Proc. Natl. Acad. Sci. U.S.A. 92*, 11666−11670.
Crowther, R. A. (1972) in *The Molecular Replacement Method* (Rossman, M. G., Ed.) pp 173−178, Gordon and Breach, New York.
Dean, A. M., & Koshland, D. E., Jr. (1990) *Science 249*, 1044−1046.
Evans, S. V. (1993) *J. Mol. Graphics 11*, 134−138.
Fauman, E. B., Rutenber, E. E., Maley, G. F., Maley, F., & Stroud, R. M. (1994) *Biochemistry 33*, 1502−11.
Garnak, M., & Reeves, H. C. (1979) *Science 203*, 1111−1112.
Gerstein, M., Lesk, A. M., & Chothia, C. (1994) *Biochemistry 33*, 6739−6749.
Hurley, J. H., Thorsness, P. E., Ramalingum, V., Helmers, N. H., Koshland, D. E., Jr., & Stroud, R. M. (1989) *Proc. Natl. Acad. Sci. U.S.A. 86*, 8635−8639.
Hurley, J. H., Dean, A. M., Sohl, J. L., Koshland, D. E., Jr. & Stroud, R. M. (1990a) *Science 249*, 1012−1016.
Hurley, J. H., Dean, A. M., Thorsness, P. E., Koshland, D. E., Jr. & Stroud, R. M. (1990b) *J. Biol. Chem. 265*, 3599−3602.
Hurley, J. H., Dean, A. M., Koshland, D. E., Jr., & Stroud, R. M. (1991) *Biochemistry 30*, 8671−8678.
Imada, K., Sato, M., Tanaka, N., Katsube, Y., & Oshima, T. (1991) *J. Mol. Biol. 222*, 725−738.
Kadono, S., Sakurai, M., Moriyama, H., Sato, M., & Hayashi, Y. (1995) *J. Biochem. 118*, 745−752.
Kraulis, P. J. (1991) *J. Appl. Crystallogr. 24*, 946−950.
LaPorte, D. C. (1993) *J. Cell. Biochem. 51*, 14−18.
LaPorte, D. C., & Koshland, D. E. J. (1982) *Nature 300*, 458−460.
LaPorte, D. C., & Koshland, D. E., Jr. (1983) *Nature 305*, 286−290.
LaPorte, D. C., Thorsness, P. E., & Koshland, D. E., Jr. (1985) *J. Biol. Chem. 260*, 10563−10568.
Miller, S. P., Karschnia, E. J., Ikeda, T. P., & LaPorte, D. C. (1996) *J. Biol. Chem. 271*, 19124−19128.
Navaza , J. (1994) *Acta Crystallogr., Sect. A A50*, 157−163.
Nimmo, G. A., & Nimmo, H. G. (1984) *Eur. J. Biochem. 141*, 409−414.
Otwinowski, Z. (1993) in *Proceedings of the CCP4 Study Weekend* (Sawyer, L., Isaacs, N., & Bailey, S., Eds.) pp 56−62, SERC Daresbury Laboratory, Warrington, U.K.
Ponder, J. W., & Richards, F. M. (1987) *J. Mol. Biol. 193*, 775−791.
Sack, J. S. (1988) *J. Mol. Graphics 6*, 244−245.
Sridharan, S., Nicholls, A., & Sharp, K. (1995) *J. Comput. Chem. 16*, 1038−1044.
Stoddard, B., Dean, A., & Koshland, D. E., Jr. (1993) *Biochemistry 32*, 9310−9316.
Stroud, R. M. (1991) *Curr. Opin. Struct. Biol. 1*, 826−835.
Stryer, L. (1988) *Biochemistry*, p 375, W. H. Freeman and Company, New York.

BI9711691